

Finite Element Analysis on Stretchable Conductive Ink Materials Structure Under Strain and Stress Behaviour

Ameeruz Kamal Ab Wahid¹, Mohd Azli Salim^{2,3,4*}, Nor Azmmi Masripan^{2,3,4}, Chonlatee Photong⁵, Adzni Md. Saad^{2,4} and Mohd Zaid Akop²

¹Jabatan Kejuruteraan Mekanikal, Politeknik Sultan Azlan Shah, Behrang Stesyen, 35950 Behrang, Perak, Malaysia

²Fakulti Kejuruteraan Mekanikal, Universiti Teknikal Malaysia Melaka, Hang Tuah Jaya, Durian Tunggal, 76100 Melaka, Malaysia

³Advanced Manufacturing Centre, Universiti Teknikal Malaysia Melaka, Hang Tuah Jaya, 76100 Durian Tunggal, Melaka, Malaysia

⁴Intelligent Engineering Technology Services Sdn. Bhd. Melaka, Malaysia.

⁵Graduate School, Mahasarakham University, Khamriang Sub-District, Kantarawichai District, MahaSarakham 44150, Thailand

ABSTRACT

Stretchable conductive ink provides an alternative for embedding electronics in garments, accessories, and medical devices. The ink can be utilized to develop a thin stretchable form-fitting circuit in wearable devices that allows for both comfort and freedom. Using maximum principal elastic strain and Von Mises stress analysis, this study determines the best materials for conductive ink performance. It was carried out with the use of finite element analysis (FEA) modelling approaches. For FEA analysis, five different materials of conductive ink straight-line pattern were developed: copper (baseline), silver, graphene, carbon black, and carbon nanotubes (CNT). The previous study's mechanical properties were applied. By evaluating the maximum principal elastic strain and equivalent stress (Von Mises stress), FEA modelling was utilized to identify which conductive ink materials had more elasticity. For the varying materials effect of the 20% elongation stress, a modelling approach of conductive inks pattern related to elasticity theories was proposed to be used. The strain and stress difference during stretching was optimized by using fatigue in the pattern line's cross-section area. Because the strain and stress values of all materials were not considerably different, there was no obvious difference in the cross-section between all conductive inks, especially in the red-coloured area. The carbon-based conductive ink of CNT and graphene achieved the best results in terms of maximum principal elastic strain with the values of 0.5320 and 0.5451, respectively with the percentage difference from copper (baseline) of 0.77% and 3.21%. Carbon black and graphene had the highest percentage difference when compared to copper (baseline), which had over 7 times less stress, with Von Mises stress values of 7,373 MPa and 8,060 MPa, respectively. This research also demonstrates that the FEA method can be used to investigate the stretchability of conductive ink.

Keywords: Stretchable conductive ink, conductive ink materials, finite element analysis, maximum principal elastic strain, Von Mises stress

1. INTRODUCTION

The present printed circuit boards (PCBs) are physically fragile and easily broken when subjected to high pressure. To overcome these problems, various conductive fillers such as gold, platinum, carbon nanotube, silver nanoparticles, organic conductive polymers and graphene have been used in printed electronics technology as a substitute to PCB technology and increase the flexibility of the circuit. PCB manufacturing infrastructure is complicated for both additive and subtractive conductor processes [1]. Other equipment such as wire connection boards are

*azli@utem.edu.my

required to produce a sensor system that employs a wire connection. Low manufacturing costs, long-term durability, environmentally friendly production processes, recyclability, lower energy usage, and improved efficiency, as well as electronic integration as part of other structures, are all essential new electronic properties [2]. The use of conductive inks has accelerated the transition from rigid, inconvenient electrodes to today's more comfortable, affordable, and disposable sensor pads. According to [3], the conductive ink was utilized as a transducer to transform pressure into an electric signal.

According to [4], stretchable substrates or electronics that can be stretched allow them to be employed in wider application space and also increase longevity. Stretchable substrates have become an important component in the circuit connection of many stretchable devices' working circuits. A high-quality stretchable printed circuit must be able to sustain electrical conductivity performance despite being exposed to high temperatures together with the substrate [5]. Connecting hard components using stretchable interconnects is a common approach in stretchable electronic design and fabrication [6]. Various stretchable electronic devices, including stretchable heaters, stretchable energy conversion and storage devices, stretchable transistors and artificial skin are manufactured with the help of a variety of manufacturing processes [7].

Stretchable electronics is a device that can be compressed, twisted, and adhered to a very complicated shape. The mechanical and electrical compliances of stretchable electronics can pave the way for health care, entertainment, and energy applications [8]. The most challenging aspect of developing materials for stretchable printed electronics is developing a printable conductor or electrode [9]. Stretchable conductive ink has been widely used in a variety of industries, including fabric, health, automotive, communications, and others. A circuit's flexibility allows it to be placed on an uneven surface or to change over time. Because the stretchy platform is always exposed to cyclic motion and deformation, it provides an advantage for widespread and unobtrusive sensor and display applications [10]. In the context of printed conductors, stretchability is defined as the percentage change in resistance of a printed conductor when exposed to induced uni-axial stress. A lesser decrease in resistance benefits stretchability [11].

Measuring mechanical strain of relative displacement or deformation is crucial for understanding the functional changes in conductive ink and clarifying basic relationships between mechanical loading and conductive ink response. When a film on a substrate is bent into a cylinder of radius R , the outside surface encounters tensile strain while the inner surface encounters compressive strain [12, 13]. The strain distribution and failure mechanisms in the entire architecture should be completely investigated during mechanical deformation and atomistic calculations can be employed to provide a guideline for device construction design [14]. It is important to understand the conductive ink content which can be determined using the cross-section measurement [15]. More conductive ink will cause more distortion, which can have a substantial impact on the results. The influence of the conductive ink materials on the strain and stress in a circuit is commonly investigated in an experimental setup. According to Hooke's law theory of elasticity, mechanical stress is directly proportional to the strain, and the biggest Von Mises stress usually occurs in the most stretchable and flexible film. The "proportionality factor" is no longer becomes a single real value due to the fact that general stresses and strains can have multiple independent components [14].

However, there is a lack of data on the induced stress by attachments, as well as the effect of different conductive ink materials and robustness on stress dissipation. Experimental results can be used as an input parameter for material properties in FEA modelling to determine the maximum principal elastic strain and equivalent stress (Von Mises stress). The strain and stress difference during stretching might be optimized by using the fatigue in the pattern line's cross-section area. This study aimed to demonstrate how stretching a screen-printed straight-line design with various conductive ink materials causes significant strain and stress variance. It can be estimated using the maximum principal elastic strain and Von Mises stress generated by FEA

modelling. Von Mises stresses were used to evaluate the stress distribution in the conductive ink patterns, as a higher Von Mises stress indicated a higher risk of failure [16]. Following the completion of the above objective, an attempt was made to determine the best-printed conductor thickness with the best stretchability using maximum principal elastic strain and Von Mises stress obtained from FEA modelling.

1.1 Previous FEA of Conductive Inks

[17] developed a graphene conductive ink formulation with several filler loading percentages to identify and select the most functional conductive ink. Graphene was used as a filler, Araldite® as an epoxy resin, and Huntsman polytheramine as a hardener in the conductive ink, all of which were used without modification. The sheet resistance values were collected using the In-Line Four-Point Probe during the electrical characterization analysis. The sheet resistance data was then analyzed to determine the volume of resistivity for FEA analysis. A sample from the electrical characterization was used for mechanical characterization analysis. Mechanical characterization studies were performed to determine the material's strength, which then can be utilized to calculate FEA mechanical properties.

Table 1 lists the properties of conductive ink derived from previous experiments, as well as the ink source. The numerical findings were compared to the experimental results. Numerical workbench tools were used to accomplish the FEA of the conductive ink pattern. The conductive ink was constructed using CATIA modelling software, then exported as an IGES file and imported into the workbench. The model was then fine-meshed, and the computing process was expected to take a decent length of time. FEA of ink stresses on a straight-line screen-printed pattern was performed with ANSYS software to simulate the strain and stress behaviour of the circuit under mechanical loads. Table 1 lists the material parameters that were used in earlier FEA studies.

Table 1 Graphene Properties Used for Simulation Analysis [17]

Materials	Properties				
	Young's Modulus (Pa)	Poisson's Ratio	Density (kg/m ³)	Thermal Conductivity (W/m °K)	Resistivity (Ω.m)
Graphene	15.49 x 10 ⁹	0.149	2200	5300	0.249

Due to its exceptional electrical, mechanical, and thermal properties, graphene as a filler has the potential to increase the efficiency, reliability, and durability of various applications for the future generation of electronic devices, composite materials, and energy storage devices [18]. Graphene has the most potential as a high-performance absorption material due to its numerous appealing qualities such as distinctive structural effects, high specific surface area, and high conductivity [19]. Graphene has been a major source of research due to its numerous appealing qualities, including excellent electrical conductivity, mechanical efficiency, and elasticity [20]. According to [17] FEA results, the straight-line pattern's stretchability after 20% elongation is 0.5451 and 8,060 MPa for maximum principal elastic strain and Von Mises stress, respectively.

Due to the high cost of materials, copper, iron, and nickel are less expensive options, but they have the problem of easily oxidizing in the air, which generates an insulating barrier on their surface [21]. Using numerical and experimental investigations, [22] studied the deformation behaviour and failure mechanisms of parallel-aligned, horseshoe-patterned, stretchy conductors encapsulated in a polymer substrate. The researchers showed that the copper stretchable conductors may elongate up to 123% and 135% without metal rupture for fine and coarse pitches, respectively, based on the experimental results. According to the researchers, the strain was 35.00 x 10⁻³ by using a mechanical model with a line to line pitch of 3.0 mm and a 20% elongation.

Silver is expensive and requires high sintering temperatures to achieve good conductivity, which limits its use on flexible substrates [23]. [24] studied the electrical and mechanical characteristics of a silver inkjet-printed patch antenna under uniaxial and biaxial bending. A 30 mm × 40 mm patch antenna with a truncated copper ground plane was designed and manufactured using inkjet printing on a polyethylene terephthalate (PET) substrate. FEA was used to determine the strain distribution during uniaxial and biaxial bending. Based on the outcomes of the FEA studies, the researchers discovered a maximum strain of 0.0169 under uniaxial bending and 0.0029 under biaxial bending.

Another conductive substance is carbon, which comes in the forms of graphite, carbon black, and carbon nanotubes (CNT) [25]. Carbon black possesses good mechanical qualities, a low specific weight, and is easy to prepare among other conductive materials. [26] explored how the mechanical performance of carbon fiber-reinforced epoxy composites was affected by different amounts of carbon black particles. In the early stages of their research, researchers were putting the composite materials they had created through tensile, flexural, and impact tests. The experimental result was validated using the numerical method. In terms of mechanical performance, the researchers discovered that carbon black/epoxy composites reinforced with carbon fibre outperformed typical carbon fiber-reinforced epoxy matrix composites. When compared to the tensile strength of conventional carbon fabric-reinforced epoxy composites, the FEA findings from the analytical tensile test were 110.43 MPa, equivalent to 65.78% improvement.

CNT has the advantage of being able to function as a metal or a semiconductor depending on its chirality, and it can withstand high temperatures [27]. [28] offer a computational technique for estimating effective orthotropic elastic properties of carbon nanotube (CNT) nanocomposites under various component conditions. The Mori-Tanaka (MT) homogenization methodology was integrated with a finite element method (FEM) approach to forecasting the effective material properties of nanocomposites. The FEA employing the hollow cylinder model yielded strain and stress values of 13.5 and 1,000 MPa, respectively. The researchers also revealed that the interface between the matrix and the filler had a significant impact on polymer composites' effective elastic strength. Previous researchers used numerous different sorts of patterns to conduct FEA studies on various conductive ink materials in order to acquire adequate strain and stress values for flexibility. Table 2 shows the strain and stress findings obtained by previous studies utilizing various conductive ink materials and designs.

Table 2 Strain and Stress Results Carried by Researchers Using Various Conductive Ink Materials and Patterns

Materials	Simulation Pattern	Maximum Principal Elastic Strain	Von Misses Stress (MPa)	Reference
Copper	Horseshoe	35.00×10^{-3}	N/A	[22]
Silver	Straight line	16.90×10^{-3}	N/A	[24]
Graphene	Straight line	545.10×10^{-3}	8060	[17]
Carbon Black	Straight line	N/A	110.43	[26]
CNT	Hollow cylinder	13.50×10^{-3}	1000	[28]

1.2 Mechanical Properties

Mechanical characteristics analysis main objective was to find the strength of a material. Nano-indentation equipment is used to assess the samples' hardness. Nanoindenter testing is based on using a high-resolution actuator to force an indenter into the test surface and a high-resolution to continually quantify the penetration that happens [29]. Because Young's modulus and the

maximum depth were feasible for this experiment, a maximum load of 150 mN was utilized based on previous experiments [17]. Since graphene can be generated cost-effectively on an industrial scale, and the graphene functional groups allow their hydrophilicity and processability of formulations, the majority of graphene and its application studies have concentrated on the reduction of graphene materials [30].

The maximum load is determined by the depth of penetration of the indenter into the surface [31]. To avoid the formulation from breaking and rupturing, and therefore losing its protective effect, the depth of the nano-indentation is carefully regulated. When measuring thin films, the indenter may penetrate too deeply if the load is too high, which the results can be influenced by the substrate's properties. The roughness of the specimen surface will influence the results if the load is too low. The elastic behaviour of printed ink is determined using the nanoindenter test. By permitting the bending or stretching of conductive ink circuits, the Young's Modulus can identify the physical parameters of the formulation. The results of this experiment were subsequently employed as an input parameter in the FEA of graphene formulation.

2. METHODOLOGY

This study aimed to determine which material would have the least amount of stress based on its percentage value. The numerical results were then compared to the experimental outcomes. The FEA of the patterns was performed using numerical workbench tools. Patterns were designed in CATIA modelling software, then converted as an IGES file and imported into the workbench. After that, the model was fine-meshed, and the computation process was expected to take some time. ANSYS software was used to simulate strain and stress behaviour of the circuit under mechanical loads utilizing FEA of ink stresses on a straight-line screen-printed pattern.

2.1 Model Configuration

Data from previous studies and FEA models were used in the research. Previous graphene material properties were used, as well as simulated maximum principal elastic strain and Von Mises stress values. The stress analysis simulations were carried out using the finite element programme ANSYS Workbench. Ink patterns with a thickness of 0.1 mm were used to generate the FEA model. Because of the symmetrical geometry in the X direction, a half model was utilized. [32] measured the lifetime of stretchable conductors under a certain strain using a 20% stretch. For this work, 20 percent elongation stress was applied uni-axially along the X-axis, as shown in Figure 1.

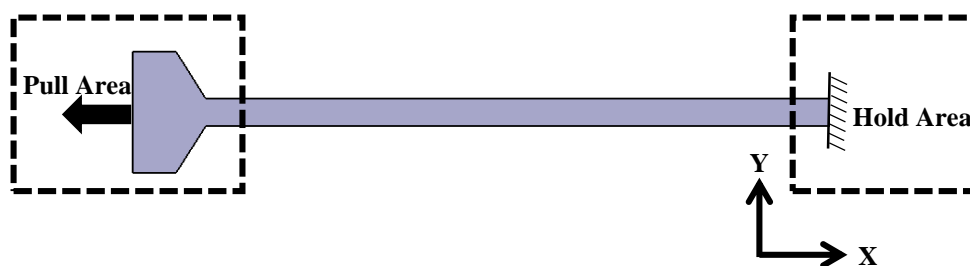


Figure 1. FEA straight-line model.

2.2 FEA

The results are determined by numerically solving the governing equations at each node using a mesh-generated finite element approach. As shown in Figure 2, the fine mesh option was used with the straight-line model preference with a longer duration of the computation process. The finite element was produced with an element size of 1.9×10^{-4} mm, resulting in 6,915 elements.

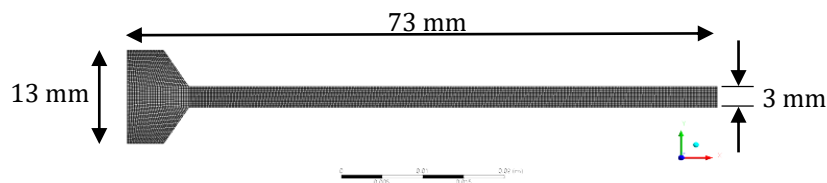


Figure 2. Mesh model of the straight-line sample.

FEA of conductive ink strains on a straight-line screen-printed pattern using ANSYS software was used to simulate the circuit's strain and stress behaviour under mechanical loads. The ink was approximated as a layered structure to imitate the screen-printing method. The study's purpose was to see how different conductive ink materials affected the printed pattern's resulting stresses. On the same substrate, the patterns were printed using the same printing and curing procedures. The focus of this research was to find out which conductive ink materials had the least amount of strain and stress based on their maximum values. Cross-sectional observations are also discussed at maximum value strain and stress points.

The material properties used for this FEA research are presented in Table 3. The values of material properties used in this paper were obtained from previous and other research studies.

Table 3 Material Properties Used for Simulation Analysis

Materials	Properties		References
	Young's Modulus (MPa)	Shear Modulus (Pa)	
Copper	110 x 10 ³	4.104 x 10 ¹⁰	[24]
Silver	95.506 x 10 ³	3.486+ x 10 ¹⁰	[33]
Graphene	15.49 x 10 ³	6.741 x 10 ⁹	[17]
Carbon Black	14.11 x 10 ³	7.055 x 10 ⁹	[26]
CNT	30.612 x 10 ³	1.177 x 10 ¹⁰	[28]

3. RESULTS AND DISCUSSION

3.1 Theoretical and Simulation-Based Results

Table 4 shows the percentage difference between copper (baseline) and other conductive ink on the maximum principal elastic strain and Von Mises stress. The strain can be approximately computed by $\epsilon = \Delta L/L$, where ϵ is the strain, ΔL is the total elongation from the neutral axis of the pattern structure and L is the original length of the pattern. The hand calculated strain with 20% elongation is 0.2012 for the straight-line pattern. The maximum principal elastic strain contours of the conductive ink were derived from numerical simulations, which were compared to the hand-calculated values for expedience. These magnitudes from all maximum principal elastic strain results as shown in Table 4 were close to the hand calculated value of 0.2012 thus validating the FEA results. The following equation was used to solve all percentage changes:

$$\% \text{ Change} = \frac{(V2-V1)}{[V1]} \tag{1}$$

where:

V1 = Theoretical maximum principal elastic strain value

V2 = Simulation maximum principal elastic strain value

Table 4 FEA Results Summary Compared with Hand Calculated Strain

Type	Material	Hand Calculated Strain / Theoretical Strain	Maximum Principal Elastic Strain	% Change In Strain
a	Copper (Baseline)	0.2011	0.5279	Increase 162.51
b	Silver		0.5245	Increase 160.82
c	Graphene		0.5451	Increase 171.06
d	Carbon Black		0.5559	Increase 176.43
e	CNT		0.5320	Increase 164.55

3.2 Comparison between Copper (Baseline) and Other Conductive Inks

Table 5 demonstrates that carbon black has the highest percentage compared to copper (baseline), followed by graphene, CNT, and silver. Carbon black has a percentage difference value of 5.17% for maximum principal elastic strain and -154.14% for Von Mises stress when compared to copper (baseline). It can also be stated that the carbon black percentage value is 5.17% higher at maximum principal elastic strain and 154.14% lower at Von Mises stress than a copper (baseline). The following equation was used to solve all percentage differences:

$$\% \text{ Difference} = \frac{(V1-V2)}{\left[\frac{(V1+V2)}{2}\right]} \quad (2)$$

where:

V1 = Other conductive ink (maximum principal elastic strain or Von Mises stress) value

V2 = Copper conductive ink (maximum principal elastic strain or Von Mises stress) value

Mechanical stress is directly related to the strain according to Hooke's law theory of elasticity, and the highest Von Mises stress results in the most stretchable and flexible conductive ink. Table 5 shows the results of the maximum principal elastic strain and Von Mises stress from different materials of conductive ink which are type (a) copper (baseline), (b) silver, (c) graphene, (d) carbon black, and (e) CNT. The numerical simulation shows that silver as a metal-based produces a result that is slightly lower than the result of other materials with 0.5245 for maximum principal elastic strain or less than 0.65% than the closest result, copper which is also a metal-based material. The FEA results also show that carbon-based materials like graphene, carbon black and CNT produce maximum principal elastic strain values of 0.5451, 0.5559 and 0.532, respectively. These insignificant differences between carbon-based materials also prove that they possess better elasticity characteristics than metal-based materials.

The Von-Mises stress value shows copper (baseline) has the highest value compared to all the materials tested. A value of 56,935 MPa indicates that copper (baseline) has a high level of hardness when subjected to pressure and does not possess high stretchability behaviour. The value of Von Mises stress for silver is 14.24% lower than copper (baseline) with 49,367 MPa. CNT Von Mises stress result of 15,866 MPa is the highest compared to other carbon-based materials followed by graphene and carbon black with the values of 8,060 MPa and 7,373 MPa respectively.

Table 5 FEA Results Summary with Percentage Differences of Conductive Inks to Copper (Baseline)

Type	Material	Maximum Principal Elastic Strain	% Difference to Baseline	Von Misses Stress (MPa)	% Difference to Baseline
a	Copper (Baseline)	0.5279	0	56935	0
b	Silver	0.5245	-0.65	49367	-14.24
c	Graphene	0.5451	3.21	8060	-150.4
d	Carbon Black	0.5559	5.17	7373	-154.14
e	CNT	0.5320	0.77	15866	-112.83

Figures 3 and 4 show a cross-section view of the condition for various conductive ink materials. When given a 20% elongation, the maximum principal elastic strain in Figure 3 shows that a metal-based conductive ink material performs better in strain. As illustrated in Figures 3 and 4, the maximum value of maximum primary elastic strain is located at the same corner as the maximum value of Von Mises stress.

As seen in Figures 3 and 4, most strain and stress occur at the sharp edge closest to the applied force of the pattern. Due to the enormous tension exerted during this hogging condition, the pattern may be catastrophically broken at the sharp edge area [34]. The highest value is highlighted in red, while the lowest value is highlighted in blue. From a cross-section view, there is no discernible difference between all conductive inks, especially in the red coloured area, because the strain and stress values of all materials are not significantly different. In Figure 3, type (d) indicates the highest strain in the model with the value of 0.5559, which indicates that it can withstand more stress than the other samples.

The straight-line pattern's center was fixed to prevent the node from moving along the x-axis. The entire pattern bent and deformed in all directions. Because the pull area in the pattern was larger than the fixed area, the component deformed or expanded at a different rate and generated stresses. A maximum value of strain and stress can be seen in the sharp edge or corner pattern. The corresponding red stresses were not visible on almost the entire side of the pattern; instead, they were at the pattern's corner. Figures 3 and 4 indicate that when the material's Young's modulus increases, the strain and stress increase. This shows that the material's Young's modulus influences strain and stress values, which can reduce failure and hence increase material flexibility. As the material thickness increases, the equivalent stress value at the corner can be reduced [15].

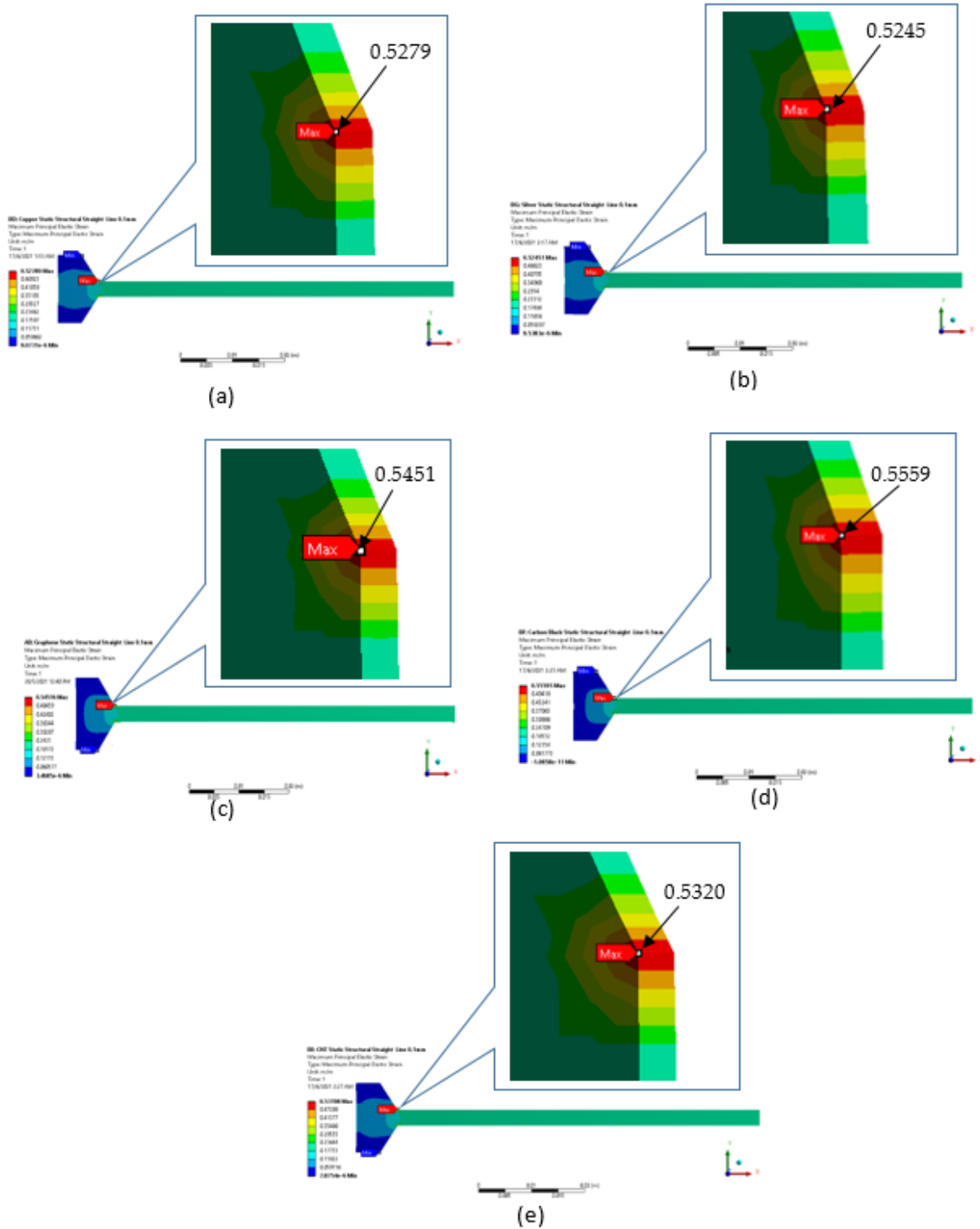


Figure 3. Maximum principal elastic strain of conductive ink materials with cross-section view. (a) Copper; (b) Silver; (c) Graphene; (d) Carbon Black; (e) CNT.

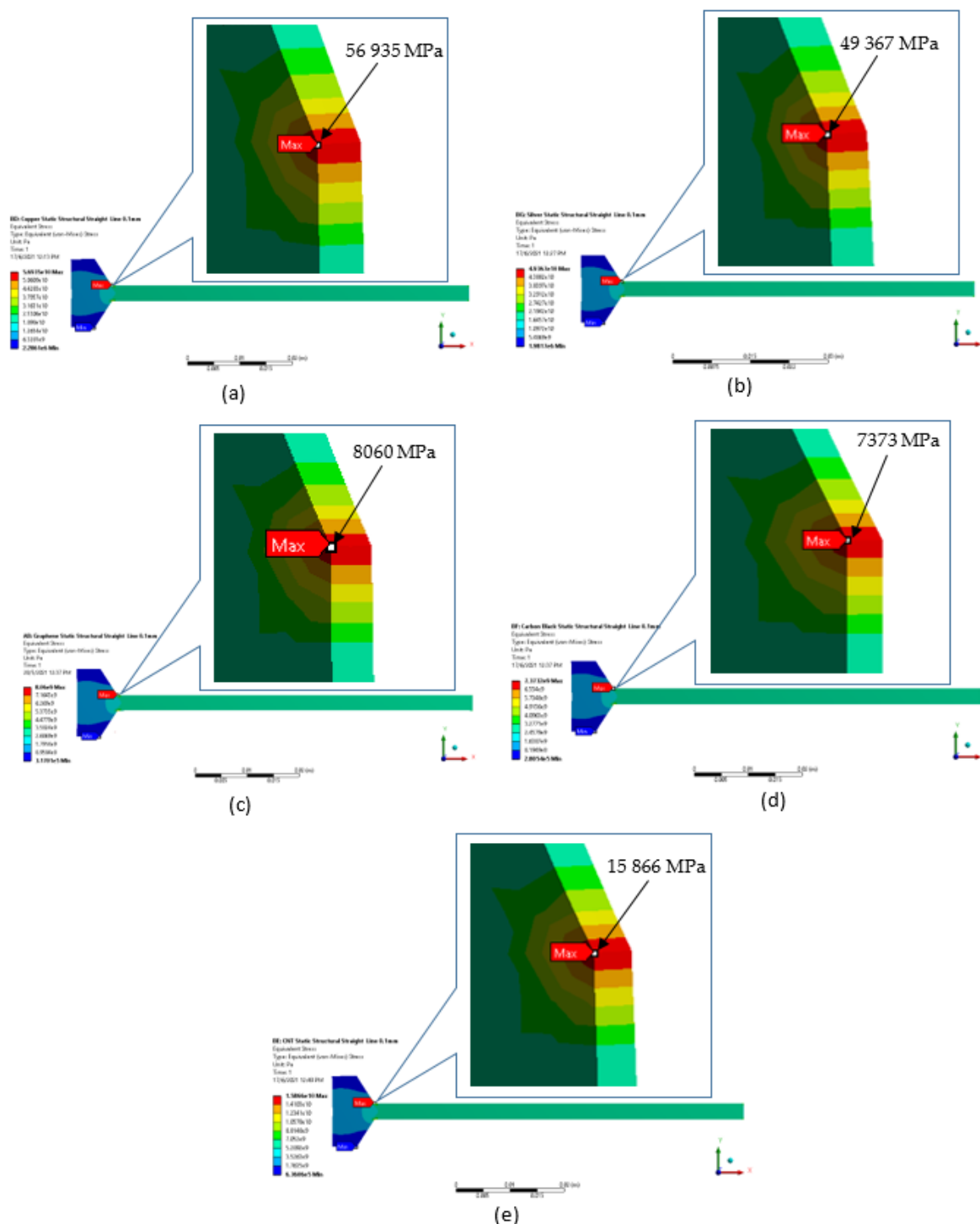


Figure 4. Von-Mises stress of conductive ink materials with cross-section view. (a) Copper; (b) Silver; (c) Graphene; (d) Carbon Black; (e) CNT.

The maximum principal elastic strain for each of the samples was determined using the FEA results, with the assumption that the samples with the lowest maximum principal elastic strain would have the best stretchability value [17]. As we can see in Figure 5, the metal-based (copper and silver) conductive inks maximum principal elastic strain are lower than carbon-based (graphene, carbon black and CNT). The maximum principal elastic strain value for type (b), silver is 0.5245, which is the lowest among the other types. Although type (e) is a carbon-based conductive ink, the maximum principal elastic strain value is 0.5320 which is slightly different

from type (a) which has a maximum principal elastic strain of 0.5279. This indicates that type (e) has a strain characteristic almost similar to metal-based materials.

Figure 6 indicates that metal-based, copper, and silver conductive inks have the highest Von Mises values of all the conductive inks. This means that metal-based conductive inks have a much higher hardness than carbon-based inks. The influence of metal-based Young's modulus, which is disproportionately high in comparison to carbon-based materials, is responsible for the high-stress value. According to [26], the higher the percentage weight of silver nanoparticles, the higher Young's modulus and hardness of the printed silver sample.

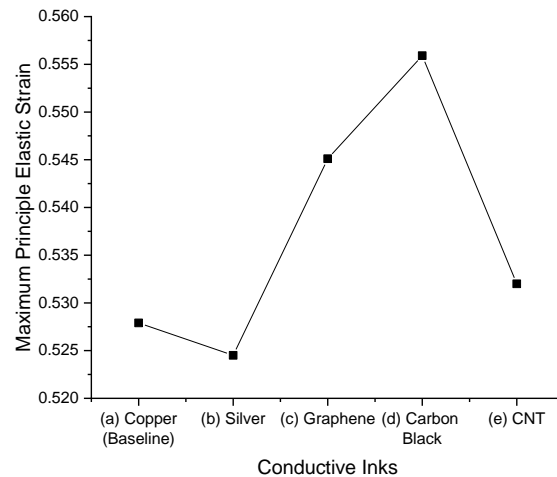


Figure 5. Maximum principal elastic strain of conductive inks.

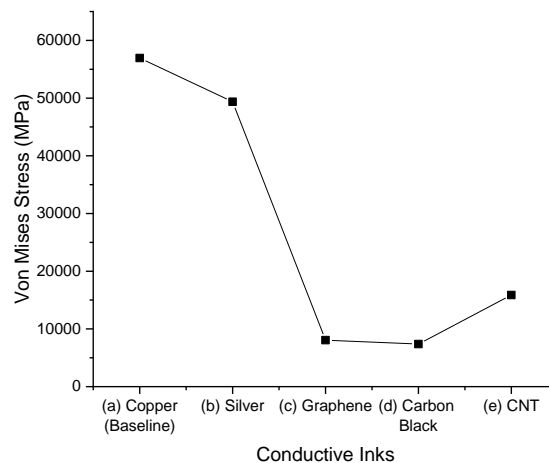


Figure 6. Von Mises stress of conductive inks.

The FEA results demonstrate that the silver has better stretchability followed by CNT as compared to copper conductive ink. Due to its low price and high conductivity, copper is a commonly used metal-based material for conductive ink applications [35]. However, copper usability is limited because copper nanoparticles can oxidize rapidly in the air, compromising their electrical properties [36]. As compared to conductive inks, the resistivity of metal foils is significantly lower [37]. After 20% strain penetration, the FEA reports that the CNT followed by graphene conductive ink is more stretchable than other carbon-based conductive inks due to its low strain and stress values. This FEA value is based on an ideal scenario with no ink-to-substrate delamination, no tension cycling, and no variations during the manufacturing process.

The type (d) in Figures 6 attains the smallest amount of Von Mises stress among all the five types of material because according to Hooke's law, the higher the modulus, the more stress is needed to create the same amount of strain. After 20% strain penetration, the FEA shows that a decrease in Von Mises stress from metal-based to carbon-based materials corresponds to 56,935 MPa to 7,373 MPa, respectively. This mechanism clearly explains the theory of elasticity defined by Hooke's law. The maximum value of Von Mises stress on the corner decreases with respect to the different types of material, as predicted by mathematical models. This FEA value is based on a perfect scenario with no ink-to-substrate delamination, no tension cycling, and no manufacturing process changes. Figures 5 and 6 show that of all the conductive inks, type (d) has the highest maximum principal elastic strain and lowest Von Mises stress values. As compared to other conductive inks, this means that it has a very high level of hardness. The high-stress value is due to the influence of type (d) modulus.

4. CONCLUSION

Using maximum principal elastic strain and Von Mises stress analysis, the study was effective in proving the optimal stretchability performance of various conductive ink materials. A modelling approach based on previous research on conductive inks patterns related to elasticity theories was developed to be applied for the varying effects of the 20% elongation stress on different conductive ink materials. Silver produced a better strain value for conductive ink in terms of maximum principal elastic strain and Von Mises stress even though it had a smaller Young's modulus than copper (baseline). The FEA indicated that the CNT followed by graphene conductive ink was more stretchable than carbon black conductive inks after 20% of strain penetration due to its low strain values. In terms of maximum principal elastic strain as a percentage difference from copper (baseline), the carbon-based conductive ink CNT and graphene, 0.5320 and 0.5451, respectively, achieved the best results, with percentage difference values of 0.77% and 3.21%.

With Von Mises stress values of 7373 MPa and 8060 MPa, respectively, carbon black and graphene had the highest percentage difference when compared to copper (baseline), which had over 7 times less stress. According to the findings, carbon black could be used as an excellent conductive ink in mechanical behaviour instead of graphene. This also verified the influence of Young's modulus values on the strain and stress behaviour of materials. The findings also revealed that FEA modelling could be utilized to produce the best stretchable screen-printed conductive ink and that the maximum principal elastic strain could be used to estimate the increase in resistance change during stretching. From the cross-section views, there was no discernible difference between all conductive inks, especially in the red coloured area, because the strain and stress values of all materials were not significantly different.

ACKNOWLEDGEMENT

Special thanks to the Advanced Manufacturing Centre (AMC) and Fakulti Kejuruteraan Mekanikal (FKM), Universiti Teknikal Malaysia Melaka (UTeM) for providing the laboratory facilities.

REFERENCES

- [1] C. Hunrath and L. Forest, "Circuit Technology Crossovers Where PCBs and Printed Electronics Meet," no. IPC APEX EXPO Conference Proceedings, (2009) p. 6.
- [2] S. Merilampi, T. Björninen, V. Haukka, P. Ruuskanen, L. Ukkonen, and L. Sydänheimo, *Microelectron. Reliab.*, vol. 50, **no. 12**, (2010) pp. 2001–2011.
- [3] J. Volf, V. Novák, and V. Ryzhenko, *Procedia Eng.*, **vol. 120**, (2015) pp. 200–205.

- [4] J. M. Nassar, J. P. Rojas, A. M. Hussain, and M. M. Hussain, *Extrem. Mech. Lett.*, **vol. 9**, (2016) pp. 245–268.
- [5] Rozali, N.S., Akop, M.Z., Sobri, N.H., Suhaimi, M.A., Azmi, M.Z., Azli, S.A., Salim, M.A., Fadzullah, S.H.S.M. and Mansor, M.R., *Proceedings of Mechanical Engineering Research Day 2018*, (2018), pp.279-280.
- [6] A. Mamidanna, Z. Song, C. Lv, C. S. Lefky, H. Jiang, and O. J. Hildreth *ACS Appl. Mater. Interfaces*, vol. 8, no. 20, (2016) pp. 12594–12598.
- [7] W. Wu, *Sci. Technol. Adv. Mater.*, vol. 20, no. 1, (2019) pp. 187–224.
- [8] E. Tan, Q. Jing, M. Smith, S. Kar-Narayan, and L. Occhipinti, *MRS Adv.*, vol. 2, no. 31–32, (2017) pp. 1721–1729.
- [9] J. Liang, K. Tong, and Q. Pei, *Adv. Mater.*, (2016) pp. 5986–5996.
- [10] Sekitani, T., Nakajima, H., Maeda, H., Fukushima, T., Aida, T., Hata, K. and Someya, T., *Nat. mater.*, **8(6)**, (2009) pp.494-499.
- [11] Zhang, B., Lei, J., Qi, D., Liu, Z., Wang, Y., Xiao, G., Wu, J., Zhang, W., Huo, F. and Chen, X., *Adv. Funct. Mater.*, **28(29)**, (2018) p.1801683.
- [12] Vosgueritchian, M., Lipomi, D.J. and Bao, Z., *Adv. Funct. Mater.*, **22(2)**, (2012) pp.421-428.
- [13] Hau, S.K., Yip, H.L., Zou, J. and Jen, A.K.Y., *Org. Electron.*, **10(7)**, (2009) pp.1401-1407.
- [14] Theogene, B., Huang, C., Cheng, Y., Ren, X., Wei, F., & Yin, H., *Ferroelectrics*, **564(1)**, (2020) pp. 113-127.
- [15] Rahangdale, U., Srinivas, R., Krishnamurthy, S., Rajmane, P., Misrak, A., Sakib, A. R., Agonafer, D., Lohia, A., Kummerl, S., Nguyen, L. T. In *2017 33rd Thermal Measurement, Modeling & Management Symposium (SEMI-THERM)* (2017) (pp. 70-76). IEEE.
- [16] Spazzin, A.O., Costa, A.R., Correr, A.B., Consani, R.L.X., Correr-Sobrinho, L. & dos Santos, M.B.F. *J. Biomech.*, **46**: (2013) 2039-2044.
- [17] AK Ab Wahid, MA Salim, M Ali, NA Masripan, F Dai & AM Saad. *Defence S&T Tech. Bull.* **14(1)**, (2021) pp. 43-54
- [18] Olabi, A.G., Abdelkareem, M.A., Wilberforce, T. & Sayed, E.T. *Renew. Sust. Energ. Rev.*, **135**: (2021) 110026.
- [19] Saad, H., Salim, M. A., Masripan, N. A., Saad, A. M., & Dai, F. *Int. J.Nanoelectr. Mater.*, **13**: (2020) 439-448.
- [20] V. Kedambaimoole, N. Neella, V. Gaddam, K. Rajanna, and M. M. Nayak, *2017 IEEE 12th Int. Conf. Nano/Micro Eng. Mol. Syst. NEMS 2017*, (2017) pp. 173–176.
- [21] Kamyshny, A. and Magdassi, S., *Chem. Soc. Rev.*, **48(6)**, (2019) pp.1712-1740.
- [22] Hsu, Y.Y., Gonzalez, M., Bossuyt, F., Axisa, F., Vanfleteren, J. and De Wolf, I., *J. Micromech. Microeng.*, **20(7)**, (2010) p.075036.
- [23] Kastner, J., Faury, T., Außerhuber, H.M., Obermüller, T., Leichtfried, H., Haslinger, M.J., Liftinger, E., Innerlohinger, J., Gnatiuk, I., Holzinger, D. and Lederer, T., *Microelectron. Eng.*, **176**, (2017) pp.84-88.
- [24] Zhou, Y., Sivapurapu, S., Chen, R., Amoli, N.A., Bellaredj, M., Swaminathan, M. and Sitaraman, S.K., *IEEE 69th Electron Compon Tech Conf (ECTC)* (2019) (pp. 1939-1945). IEEE.
- [25] Lebedev, S.M., Gefle, O.S., Dneprovskii, S.N. and Amitov, E.T., *Russ. Phys. J.*, **57(10)**, (2015) pp.1423-1427.
- [26] Chauhan, S. and Bhushan, R.K., *Adv. Compos. Hybrid Mat.*, **1(3)**, (2018) pp.602-611.
- [27] G. Cummins and M. P. Y. Desmulliez, *Circuit World*, vol. 38, no. 4, (2012) pp. 193–213.
- [28] Arora, G. and Pathak, H., *Compos Part B-Eng*, **166**, (2019) pp.588-597.
- [29] Mokhlis, M. A Study On Mechanical and Electrical Properties of Hybridized Graphene-Carbon Nanotube Filled Conductive Ink, Master Dissertation, Universiti Teknikal Malaysia Melaka, (2020).
- [30] Tran, T.S., Dutta, N.K. & Choudhury, N.R. *Adv. Colloid Interfac.*, **261**: (2018) pp. 41-61.
- [31] Batakliiev, T., Georgiev, V., Ivanov, E., Kotsilkova, R., Di Maio, R., Silvestre, C. & Cimmino, S. *J. Poly. Sci.*, **136**: (2019), 47260.
- [32] Mohammed, A.A. *Development of a New Stretchable and Screen Printable Conductive Ink*, Doctoral dissertation, University of Maryland, Maryland. (2017).

- [33] Vasiljevic, D.Z., Menicanin, A.B. and Zivanov, L.D., In *Doctoral Conference on Computing, In Doct Conf on Comp, Electr and Ind Syst* (2013) (pp. 133-141). Springer, Berlin, Heidelberg.
- [34] Rahman, M. Muzibur, Rajia Sultana Kamol, and Reyana Islam. *AIP Conference Proceedings*. Vol. 1919. No. 1. AIP Publishing LLC, (2017).
- [35] Wang, B.Y., Yoo, T.H., Song, Y.W., Lim, D.S. and Oh, Y.J., *ACS Appl. Mater. Inter.*, **5(10)**, (2013) pp.4113-4119.
- [36] Yang, W. *Preparation and characterization of organic silver based conductive inks for flexible electronics* (Doctoral dissertation, Heriot-Watt University) (2019).
- [37] Li, X., Sidén, J., Andersson, H., Sawatdee, A., Öhman, R., Eriksson, J. and Genchel, T., *Flex. Print. Electr.*, **4(4)**, (2019) p.045007.